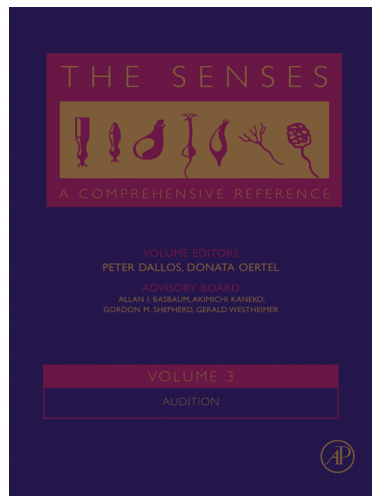


Provided for non-commercial research and educational use.
Not for reproduction, distribution or commercial use.

This article was originally published in the *The Senses: A Comprehensive Reference*, published by Elsevier, and the attached copy is provided by Elsevier for the author's benefit and for the benefit of the author's institution, for non-commercial research and educational use including without limitation use in instruction at your institution,



sending it to specific colleagues who you know, and providing a copy to your institution's administrator.

All other uses, reproduction and distribution, including without limitation commercial reprints, selling or licensing copies or access, or posting on open internet sites, your personal or institution's website or repository, are prohibited. For exceptions, permission may be sought for such use through Elsevier's permissions site at:

<http://www.elsevier.com/locate/permissionusematerial>

R M Burger and E W Rubel, Encoding of Interaural Timing for Binaural Hearing. In: Allan I. Basbaum, Akimichi Kaneko, Gordon M. Shepherd and Gerald Westheimer, editors *The Senses: A Comprehensive Reference*, Vol 3, Audition, Peter Dallos and Donata Oertel. San Diego: Academic Press; 2008. p. 613-630.

3.35 Encoding of Interaural Timing for Binaural Hearing

R M Burger, Lehigh University, Bethlehem, PA, USA

E W Rubel, University of Washington, Seattle, WA, USA

© 2008 Elsevier Inc. All rights reserved.

3.35.1	Overview and Background	613
3.35.1.1	Interaural Time Disparity: The Cue for Low-Frequency Sound Localization	614
3.35.1.2	Processing Interaural Time Disparities: The Jeffress Model	615
3.35.1.3	Processing Interaural Time Disparities: Physiology	615
3.35.2	Interaural Time Disparity Processing in Birds	616
3.35.2.1	Inputs to Nucleus Laminaris	616
3.35.2.2	Encoding of Interaural Time Disparities in Nucleus Laminaris	618
3.35.2.3	Intrinsic Properties of Nucleus Laminaris Neurons Specialized for Interaural Time Disparity Computation	619
3.35.2.4	The Role of Inhibition in Nucleus Luminaris Function	621
3.35.3	Interaural Time Disparity Processing in the Medial Superior Olive	623
3.35.3.1	Mammalian Interaural Time Disparity-Encoding Circuitry	623
3.35.3.2	Response Properties of Medial Superior Olive Neurons	624
3.35.3.3	Intrinsic Properties of Medial Superior Olive Neurons	625
3.35.3.4	The Role of Inhibition in the Medial Superior Olive	625
3.35.3.5	The Neural Code for Interaural Time Disparity in Mammals	626
3.35.4	Summary and Conclusion	627
References		627

Glossary

avian Of or pertaining to birds.

azimuth The angular distance or position in the horizontal plane.

delay line A component of either a model or physical circuit that introduces time delays into a processing unit where time delay is proportional to the length of the component.

dichotic The binaural presentation of stimuli that differ in one or more aspects (i.e., frequency, intensity, etc.).

diotic The binaural presentation of identical stimuli to the two ears.

interaural phase disparity The difference in stimulus phase at the two ears, which varies with interaural time disparity for freefield stimuli.

interaural intensity disparity The difference in stimulus intensity measured at the two ears, the magnitude of which depends on physical features of the listener, such as head size, and stimulus frequency.

interaural time disparity The difference in arrival time for a particular sound stimulus at the two ears, the magnitude of which depends primarily on head size and the speed of sound in the medium.

K_{HT}^+ High-threshold potassium conductance through a membrane, usually associated with Kv3 family potassium channels.

K_{LVA}^+ Low-threshold potassium conductance through a membrane, usually associated with Kv1 family potassium channels.

3.35.1 Overview and Background

Binaural hearing provides important perceptual information for localizing acoustic information in space and for enhancing signal-to-noise characteristics,

especially in noisy environments. Interaural time disparities (ITDs) are the principal cue animals use to localize low-frequency sounds in the azimuthal plane (horizon). In reptiles, birds, and mammals specialized regions in the auditory brainstem are devoted to

processing this cue (Carr, C. E. and Code, R. A., 2000; Carr, C. E. and Soares, D., 2002). These regions express specializations for temporal processing at the network, synaptic, and cellular levels, providing striking examples of neural architecture and molecular properties that are clearly related to the function of the circuit and the behavior for which it is utilized. Some of the features of the specialized synaptic physiology in these pathways have been discussed in previous chapters. This chapter will focus primarily on the input pathways and intrinsic properties of neurons in nucleus laminaris (NL) and the medial superior olive (MSO), binaural brainstem nuclei in birds and mammals that first process ITDs. These regions provide some of the clearest examples in neurobiology of how neuronal circuits perform computations.

Our discussion will first explore the nature of ITD cues highlighting some early historical contributions in the field, and we will review the current state of knowledge regarding the anatomy and physiology of both NL and MSO circuitry. We will focus on inhibitory components of both systems, because while inhibition has long been recognized as an important component of ITD processing circuitry, recent work has generated renewed interest in resolving its contribution to ITD processing.

3.35.1.1 Interaural Time Disparity: The Cue for Low-Frequency Sound Localization

The difference in the arrival time of sound to each ear varies systematically with a sound source's position in space along the azimuth (Figure 1(a)). A particular ITD value depends on: (1) the acoustic distance between the ears (interaural distance), (2) the speed of sound in air (or water), and (3) the angle of incidence of the sound to the listener. For example, a sound source emanating from a position in space on the midline with respect to the listener arrives at both ears simultaneously yielding an ITD of $0\ \mu\text{s}$. This value will systematically increase as the sound is shifted laterally such that a sound source at roughly 90° to the midline will lead in the ipsilateral ear by the maximal ITD, a value that is generally determined by the distance between the two ears. For humans the maximal ITD is $\sim 700\ \mu\text{s}$ (Wightman, F. L. and Kistler, D. J., 1993), while for small mammals such as the gerbil it is $\sim 130\ \mu\text{s}$ (Maki, K. and Furukawa, S., 2005).

These ITDs result in stable interaural phase differences (IPDs) for ongoing periodic sounds such as

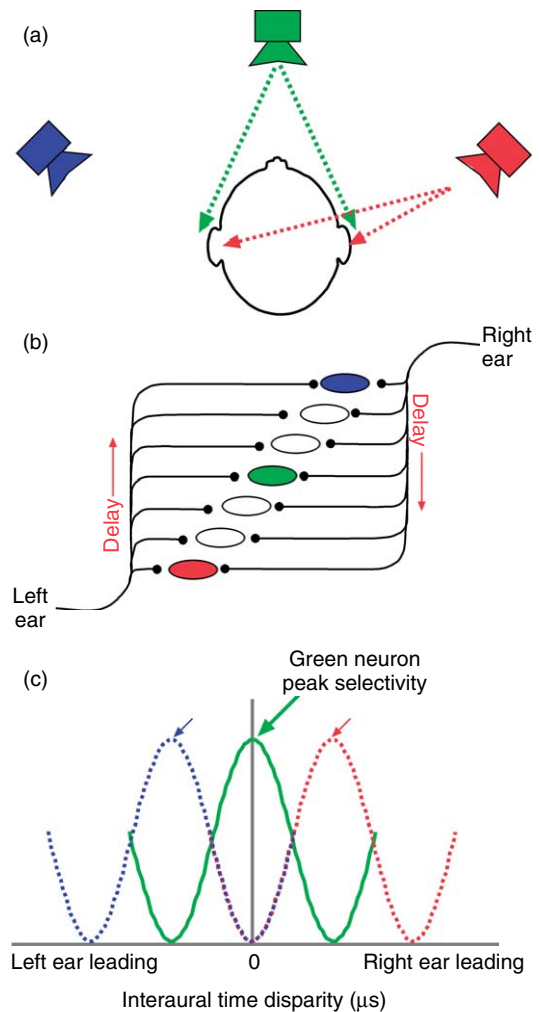


Figure 1 Illustration of the fundamental principles of ITD processing. (a) ITD varies systematically with sound source position. Three sound sources are represented by the three colored speakers. The sound path from the green speaker positioned on the midline is equidistant to each ear, resulting in an ITD of $0\ \mu\text{s}$. The blue and red speakers will lead in the left and right ears respectively and thus generate large ITDs. The maximum ITD for a human listener is about $700\ \mu\text{s}$. (b) The Jeffress model for processing ITDs. The ovals represent an array of coincidence detecting neurons and the black lines indicate the input axons to the coincidence detectors. The crucial feature is the increase in axon length (delay lines) from each ear across the array of coincidence detectors. The axon length gradient ensures that each cell in the array is maximally activated at a particular ITD with a value that is determined by the intrinsic delay of the input circuitry. The green neuron, with equal length input axons is selective for an ITD value of $0\ \mu\text{s}$, while the blue and red neurons prefer ITDs that favor the left and right ear (blue and red sound source positions), respectively. (c) The neural response functions are schematically shown for each of the three colored neurons from panel (b).

tone stimuli. The ongoing phase differences resulting from ITDs provide the principal cue animals use to localize low-frequency sounds in space. The phase difference generated at a given ITD will depend on the frequency of the stimulus. Low-frequency (long wavelength) stimuli generate relatively small IPDs. As frequency increases, the wavelength of the stimulus decreases, thus a greater change in phase (or IPD) will occur per unit time (ITD). Figure 2 illustrates this principle. For simplicity, we will refer to the auditory cue as ITD unless specifically discussing phase. The salience of ITD as a cue for sound location was demonstrated in the early 1900s by Rayleigh L. S. (1907).

Rayleigh's observations defined what is now referred to as the duplex theory of sound localization (Rayleigh, L. S., 1907; Colburn, H. S. and Durlach, N. I., 1978). The duplex theory states that sounds are lateralized on the basis of differences in both arrival time and intensity at the two ears. Arrival time cues are useful at low frequencies where wavelengths are broad and sound intensity is not significantly attenuated by the head. At higher frequencies, when wavelengths are smaller than the interaural distance (roughly 1500 Hz for humans), sound is attenuated by its interaction with the head generating substantial interaural spectral differences (intensity differences, IIDs) between the two ears. ITDs and IIDs are processed in separate parallel pathways that appear to interact through the inhibitory circuitry in both mammals and birds. The circuitry for processing

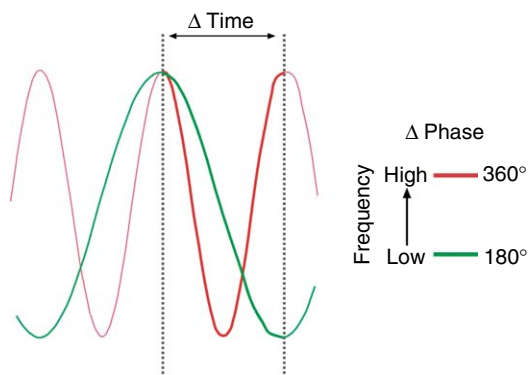


Figure 2 Illustration of the relationship between ITD and IPD. A given ITD defined by the gray dashed lines yields IPDs bold lines that depend on stimulus frequency. In this simple example, the high-frequency stimulus red waveform has a change in phase of 360° for this ITD while the low-frequency green waveform (half the frequency of the red stimulus) has a change in phase of only 180° with the same ITD.

IIDs is beyond the scope of this chapter, but is discussed in Chapter 3.36 (Pollak, G. D. *et al.*, 2002; Pollak, G. D. *et al.*, 2003; Tollin, D. J., 2003).

3.35.1.2 Processing Interaural Time Disparities: The Jeffress Model

With the acoustic cues necessary for localizing sounds in azimuth well established, a second major contribution to the field was made by Lloyd Jeffress (1948). He conceived a simple model for the computation of ITDs that has been perhaps the most enduring and influential model in auditory neuroscience. The Jeffress model comprises two major components (Figures 1(b) and 1(c)). The first is an array of coincidence detecting binaural neurons. These neurons require simultaneous or near-simultaneous input from each ear to evoke a maximal response. The second component of his model is a particular arrangement of input axons to the coincidence detectors. The inputs are arranged such that input from a given ear innervates each successive coincidence detector in the array with increasing axon lengths, thus establishing an orderly series of delay lines. A complimentary delay line array is provided by circuitry from the contralateral ear. The model's opposing sets of delay lines compensate for interaural delays such that each consecutive coincidence detecting neuron is optimally responsive to a particular interaural delay and thus systematically shifting locations in space.

3.35.1.3 Processing Interaural Time Disparities: Physiology

These early works by both Raleigh and Jeffress set the stage for decades of behavioral and physiological auditory research. Several studies in the 1960s began to explore auditory brainstem regions that exhibited binaural interactions suggestive of sensitivity to ITD (Hall, J. L., 2nd, 1965; Moushegian, G. *et al.*, 1967; Goldberg, J. M. and Brown, P. B., 1969). Among the most significant of these early pioneering studies was that of Goldberg J. M. and Brown P. B. (1969). Their work represents the first comprehensive physiological study of the MSO. MSO neurons responded primarily to low-frequency stimuli and were remarkably sensitive to ITDs. The authors showed that MSO neurons had spike rates that varied several fold over just a few hundred microseconds shifts in ITD, revealing some of the most temporally sensitive neurons ever observed in the nervous system.

Furthermore, Goldberg and Brown showed that the ITD to which the neurons were most sensitive, referred to as the neuron's "best ITD," was predictable on the basis of the latency of excitatory input from each ear. In other words, the MSO neurons were optimally driven when the time between the ears was adjusted so that the intrinsic delays from the inputs from each ear arrived simultaneously at the MSO neuron. This finding solidified support for the delay line concept proposed by Jeffress and demonstrated that neurons in the mammalian brain are selective for particular ITDs, the localization cue established by Raleigh.

Further investigation of this system in mammals as diverse as cats, kangaroo rats, gerbils, and rabbits has supported and expanded on the major findings of Goldberg and Brown (Hall, J. L., 2nd, 1965; Moushegian, G. *et al.*, 1967; Moushegian, G. *et al.*, 1975; Yin, T. C. and Chan, J. C., 1990; Spitzer, M. W. and Semple, M. N., 1995; Batra, R. and Fitzpatrick, D. C., 1997; Batra, R. *et al.*, 1997b; 1997a). Indeed, the processing of ITDs of airborne sounds appears to be a general feature of auditory systems including insects, reptiles, birds, and mammals (Hoy, R. R. and Robert, D., 1996; Robert, D. *et al.*, 1996; Carr, C. E. *et al.*, 2001). The most comprehensive literature on ITD processing has arisen from studies in birds where behavioral, anatomical, and physiological studies offer a relatively complete picture of sound localization circuitry in the auditory system.

3.35.2 Interaural Time Disparity Processing in Birds

The components of the avian auditory pathway devoted to processing interaural time cues compose what is arguably one of the most elegant and well-understood circuits in the vertebrate nervous system. The elegance of this circuit derives from the remarkable correspondence between its functional role and its anatomical and physiological characteristics. NL is the first nucleus in the avian brainstem to receive information from the two ears and appears to be the initial region where sound location is computed. In addition, it appears that both ITDs and sound frequency are mapped along orthogonal directions in NL.

Current understanding of this circuit relies primarily on studies of two species, the chicken and barn owl. Fortuitously, the data acquired from studies of each species are largely complimentary because the

attributes of each preparation are optimal for different but overlapping methods of investigation. For example, studies of the chicken have yielded exceptionally detailed developmental, cell physiological, and anatomical data, whereas the barn owl's remarkable sound localization related behavior has contributed much in relating anatomical and *in vivo* physiological observations to psychophysical and behavioral studies. The general features common to both species will be discussed, but a few of the differences will be highlighted.

3.35.2.1 Inputs to Nucleus Laminaris

In birds, sound is transduced by hair cells of the basilar papilla and relayed to the central nervous system by the auditory nerve (nVIII). nVIII fibers enter the brainstem and bifurcate to innervate two cochlear nuclei (Figure 3). The first, nucleus angularis (NA) is not directly involved in temporal coding, but does interact with this circuit through its connections with inhibitory inputs (see below). The second is nucleus magnocellularis (NM) where large endbulb of Held synaptic complexes from 2 to 4 nVIII fibers make direct contact with the somata of NM cells. This unusually secure synaptic connection preserves the spike timing information encoded in the nVIII and represents one of the early specializations in the ITD coding pathway in birds. There is

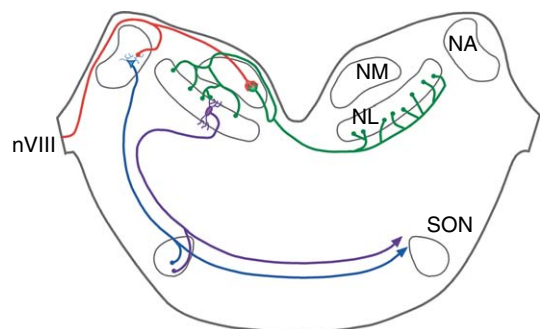


Figure 3 Excitatory pathways in the avian brainstem ITD-processing pathway. Information from the ear is conveyed over the nVIII red line to two cochlear nuclei, nucleus angularis (NA), and nucleus magnocellularis (NM). In NM the nVIII makes large endbulb of Held synapses onto the NM neurons. NM cells in turn project bilaterally to NL green projection. The NM projections to NL are the source of internal delays for ITD processing in birds. Both NA and NL blue and purple lines project to higher-order auditory centers including a fourth brainstem nucleus, the SON. The SON is the primary source of inhibition to all of the brainstem auditory nuclei.

now a vast literature on the nature of this synapse, although much of it is beyond the scope of this chapter. Excellent reviews are presented in Chapter 3.33 and in the writings of Oertel D. (1997) and Trussell L. O. (1997; 1999).

NM cell axons project bilaterally to a third nucleus, NL, the first center to receive binaural input. As with NM, NL is tonotopically organized such that neurons receiving low-frequency NM input are located at the caudolateral pole while high-frequency cells are located rostromedially (Rubel, E. W. and Parks, T. N., 1975). In the chicken, throughout most of its extent, NL is composed of a monolayer of neurons, the exception being the low-frequency caudolateral region which is a few cells thick.

The pattern of NM inputs to NL is a critical feature for the ITD-processing function of NL. Each NM cell axon branches upon exiting the nucleus medially. The ipsilateral branch arcs dorsally, passes back through the nucleus, and then courses rostrally before dipping ventrally to ramify along the dorsal dendrites and on the cell bodies of an isofrequency sheet of NL neurons. Physiological and anatomical studies have shown that the axon length to the ipsilateral NL neurons is equivalent along the isofrequency dimension (Young, S. R. and Rubel, E. W., 1983; Overholt, E. M. *et al.*, 1992). The contralateral collateral from the same NM neuron extends across the midline and branches several times to create an orderly, serial set of axonal branches extending along an analogous isofrequency band of NL neurons. These contralateral collaterals innervate the ventral dendrites and cell bodies of NL neurons within an isofrequency band (Young, S. R. and Rubel, E. W., 1983). This arrangement of innervation, predominantly along the medial to lateral dimension, results in medial laminaris cells receiving contralateral input with the shortest input axons and lateral NL cells the longest. The systematic increase of axon lengths across the nucleus effectively establishes a series of delay lines that compensate for interaural time delays. This corresponds remarkably well to the Jeffress model. One notable exception is that in the chicken NL, the delay line arises solely from the contralateral ear input, rather than bilaterally. Thus, neurons in the lateral NL will respond most vigorously to sounds with ITDs that lead in the contralateral ear (sounds that emanate from contralateral sound fields) and medial laminaris neurons that have receptive fields near the midline. Thus, each

NL topographically maps a sound field composed primarily of the contralateral sound field.

The orderly arrangement of input axons across the roughly medial to lateral dimension defines a topography of contralateral delay within NL. Orthogonal to this axis is the tonotopic axis that runs caudolaterally to rostromedially at about 30° to the sagittal plane. Precisely along this tonotopic axis, chicken NL neurons express a gradient of dendrite length (Figure 4) (Smith, D. J. and Rubel, E. W., 1979). In mature animals, dendrite length varies 11-fold from the low- to high-frequency poles of NL (Smith, D. J. and Rubel, E. W., 1979). Low-frequency cells have one or two long primary dendrites that branch profusely, while high-frequency cells have a few short ones. The possible role of this intriguing feature of NL will be discussed in Section 3.35.2.4.

The NL of the barn owl is similar to that described in the chicken, with a few important differences. First, in the high-frequency portion of NL, dendrites of mature barn owl NL neurons are short and are not restricted to the dorsal and ventral poles of the neurons (Carr, C. E. and Boudreau, R. E., 1996; Kubke, M. F. *et al.*, 2002). This may be related to the unusual ability of the barn owl to process ITD information for much higher-frequency signals than other birds and most other mammals (see below). ITDs remain a useful cue up to about 9 kHz and the owl's greatest ITD selectivity is in the range of 4–8 kHz (Knudsen, E. I. and Konishi, M., 1979). A second major difference between the barn owl and chicken is that the barn owl NL is several hundred μm thick and composed of layers of neurons throughout its extent. The input axons to these neurons enter the nucleus at the dorsal or ventral surface and course perpendicularly to the mediolateral trajectory of input axons from the contralateral NM (Carr, C. E. and Konishi, M., 1990). This arrangement of input axons through several layers of NL neurons will be discussed in Section 3.35.2.2, but it represents an expansion of the sound-localization circuitry in this predator, presumably specialized for acoustically localizing prey in the dark.

In addition to the orderly pattern of excitatory inputs to NL, GABAergic inhibitory inputs are abundant (Carr, C. E. *et al.*, 1989; Code, R. A. *et al.*, 1989; Lachica, E. A. *et al.*, 1994; Burger, R. M. *et al.*, 2005). These arise from two sources, a small population of multipolar neurons residing in the neuropil between NM and NL and a prominent projection from the ipsilateral superior olivary nucleus (SON) (von Bartheld, C. S. *et al.*, 1989; Lachica, E. A. *et al.*, 1994;

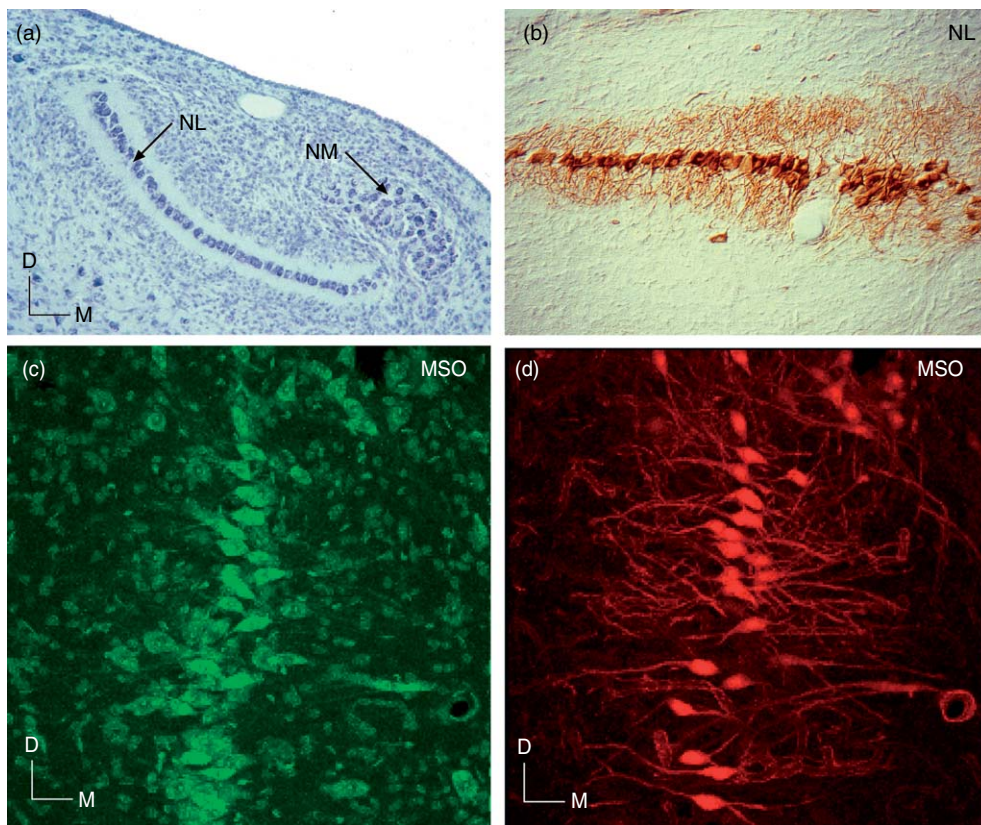


Figure 4 Comparison of NL and MSO neurons. (a) A Nissl-stained section through the auditory brainstem of the chicken showing the laminar structure of NL and the neighboring ipsilateral NM. (b) The dendrite length gradient in NL can be clearly observed in the section through NL stained for MAP2 antigen. Higher best frequency neurons are to the left, lower BF NL cells are to the right. Additionally, one can appreciate the dorsoventrally oriented bipolar dendrites. (c) Neurons of the Gerbil MSO can be seen clustered along a dorsoventral running axis in this fluorescent Nissl-stained section. (d) The bipolar mediolaterally oriented dendrites of rhodamine conjugated dextran-labeled MSO neurons in the same section as that shown in (c).

Westerberg, B. D. and Schwarz, D. W., 1995; Yang, L. *et al.*, 1999; Burger, R. M. *et al.*, 2005). The functional impact of this inhibitory input has been the focus of intense study and current understanding of inhibition's role in the computation of ITDs will be discussed in some detail further in this chapter.

3.35.2.2 Encoding of Interaural Time Disparities in Nucleus Laminaris

NL's primary function appears to be the computation and topographic representation of ITDs across the nucleus. The most compelling data available on a topographic ITD representation has derived from studies of the barn owl nucleus laminaris and *in vitro* data from the chicken (Parks, T. N. and Rubel, E. W., 1975; Sullivan, W. E. and Konishi, M., 1986; Carr, C. E. and Konishi, M., 1990; Overholt, E. M. *et al.*, 1992; Joseph, A. W. and Hyson, R. L., 1993). The

suggestion that innervation pattern of NL from the contralateral NM may represent a Jeffress-type delay line was first suggested for the chicken by Parks T. N. and Rubel E. W. (1975) where the topography of these connections was initially described. Later physiological and anatomical work in both the barn owl and chicken has confirmed the hypothesis of Parks T. N. and Rubel E. W. (1975).

While the anatomical substrate of the delay line that generates the topographic representation was identified and described in the chick by Young S. R. and Rubel E. W. (1983) (Figure 5), the contribution of delay lines to the resultant topographic representation of ITD was demonstrated physiologically *in vivo* by a sequence of papers from the Konishi lab (Sullivan, W. E. and Konishi, M., 1986; Carr, C. E. and Konishi, M., 1990). In the first paper, roughly dorsal to ventral electrode penetrations were made through NL transecting the contralateral NM axon

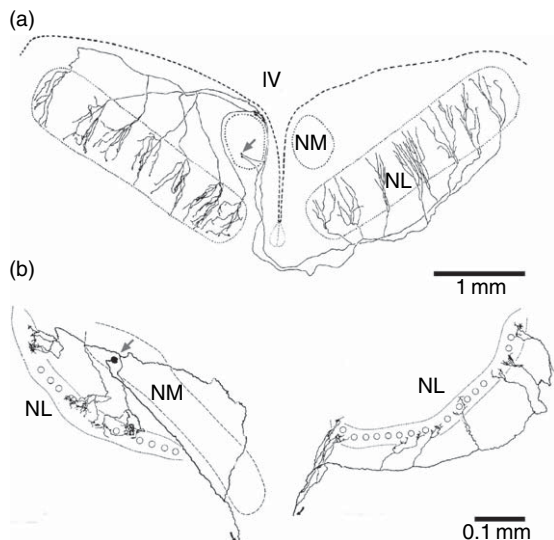


Figure 5 A comparison of the inputs from NM to NL in the barn owl and chicken reveals the exquisite architecture of the avian ITD-coding system. (a) Reconstruction of projections from two barn owl NM neurons to their targets in NL and in (b) reconstruction of an NM neuron projection in the chicken. In both barn owl and chicken, the contralateral projections innervate medial NL neurons with the shortest axon segments while the lateral NL cells receive the longest NM axon length inputs. In the barn owl, the orderly and opposing innervation from the dorsal and ventral borders of NL by NM axons may lead to additional sources of delay. NM neuron somas are labeled by gray arrows in both panels. (a) From Carr, C. E. and Konishi, M. 1990. A circuit for detection of interaural time differences in the brain stem of the barn owl. *J. Neurosci.* 10, 3227–3246. (b) From Young, S. R. and Rubel, E. W. 1983. Frequency-specific projections of individual neurons in chick brainstem auditory nuclei. *J. Neurosci.* 3, 1373–1378.

length gradient obliquely. Sullivan W. E. and Konishi M. (1986) demonstrated that as the electrode advanced ventrally (and roughly across the gradient of medial to lateral input axon lengths) the ITD for eliciting a maximum field potential shifted systematically toward the contralateral ear.

A later study by Carr C. E. and Konishi M. (1990) in which recordings were made from NM axons in addition to NL cells, demonstrated that when electrode penetrations were made perpendicular to the mediolateral running plexus of NM input axons in the ventral NL, delays increased or decreased with depth, depending on whether the axon was from ipsilateral or contralateral NM, respectively. In addition, a given interaural phase delay was often represented more than once in a single penetration. These authors have suggested that in the barn owl,

the topographic representation of the entire range of ITDs is represented along the dorsal–ventral axis of NL, and this representation is repeated many times along the predominantly mediolateral dimension that is orthogonal to the tonotopic dimension. In other words, the layered expansion of NL in barn owls could generate an additional source of delay lines not present in other bird species.

The presence of delay lines in the bird auditory pathway was directly demonstrated by *in vitro* chick brainstem slice studies in the Rubel lab (Overholt, E. M. *et al.*, 1992; Joseph, A. W. and Hyson, R. L., 1993). Hyson and colleagues recorded postsynaptic field potentials from NL neurons while systematically shifting the timing of stimulated inputs from the ipsilateral and contralateral NM. In these studies, a dramatic difference was observed when stimulating the ipsilateral versus contralateral input to NL neurons. Increasing delays were observed as the electrode was moved along an isofrequency line of NL neurons; that is, rostrolaterally parallel to the main axis of input axons thus confirming the source of input delays. Consistent with predictions from the anatomical observations of Young S. R. and Rubel E. W. (1983), latencies of the postsynaptic responses to ipsilateral stimulation did not vary as the electrode is moved from medial to lateral. On the other hand, the latencies of postsynaptic responses to contralateral stimulation systematically increased along the delay line dimension. Furthermore, these studies showed that NL cells were most optimally driven by binaural inputs timed to compensate for the mismatch in delay from each NM.

3.35.2.3 Intrinsic Properties of Nucleus Laminaris Neurons Specialized for Interaural Time Disparity Computation

The studies reviewed above provided the anatomical and physiological groundwork for a next generation of studies that have explored the unique specializations of intrinsic physiological properties in NM and NL that contribute to ITD calculations. Perhaps the most ubiquitous attribute of neurons involved in processing temporal aspects of auditory stimuli is the prevalence of potassium conductances that are suited to enhance temporal encoding. These include both a low-threshold potassium conductance (K_{LVA}^+) associated with Kv1 family channel subunits and a high-threshold (K_{HT}^+) conductance associated with Kv3 family channel subunits.

The K_{LVA}^+ conductances have been investigated in a large number of auditory neurons (Oertel, D., 1983; Manis, P. B. and Marx, S. O., 1991; Banks, M. I. and Smith, P. H., 1992; Reyes, A. D. *et al.*, 1994; Zhang, S. and Trussell, L. O., 1994; Brew, H. M. and Forsythe, I. D., 1995; Smith, P. H., 1995; Reyes, A. D. *et al.*, 1996; Rathouz, M. and Trussell, L., 1998; Bal, R. and Oertel, D., 2001; Adamson, C. L. *et al.*, 2002; Svirskis, G. *et al.*, 2002; Svirskis, G. *et al.*, 2003; Kuba, H. *et al.*, 2005; Scott, L. L. *et al.*, 2005). The channels underlying this conductance are activated at voltages at or just above rest and have several influences on information processing. First, the strong outward conductance causes a reduced membrane input resistance thus shortening the time constant of the membrane. This has the dual effect of reducing the time course of voltage changes from a given input and correspondingly reducing the time window during which inputs can summate. Second, these neurons typically respond to sustained depolarizing currents with a single action potential, allowing the membrane to recover quickly from an excitatory input. This property has been observed in many auditory neurons in a mammalian medial nucleus of the trapezoid body (MNTB) neuron from a study by Brew H. M. and Forsythe I. D. (1995) is shown in Figure 6. A third effect of this conductance is to raise the neuron's threshold. Together, these effects may increase the requirement for inputs to be coincident in order to evoke a postsynaptic action potential, a property which provides improved temporal processing ability advantageous for the encoding of ITDs (Carney, L. H., 1992; Rothman, J. S. *et al.*, 1993).

The channels underlying the K_{HT}^+ conductances activate at high voltages in the range of -20 mV and thus may only be activated by action potentials (Gan, L. and Kaczmarek, L. K., 1998; Rudy, B. and McBain, C. J., 2001). These channels' protein subunits or their mRNAs have been shown to be highly expressed in both NL and NM (Parameshwaran, S. *et al.*, 2001; Parameshwaran-Iyer, S. *et al.*, 2003; Lu, Y. *et al.*, 2004), as well as in mammalian time-coding neurons (Perney, T. M. *et al.*, 1992; Perney, T. M. and Kaczmarek, L. K., 1997; Grigg, J. J. *et al.*, 2000). The K_{HT}^+ conductances confer upon neurons the ability to rapidly repolarize following an action potential and thus the primary role of K_{HT}^+ currents appears to be the preservation of high-frequency firing (Brew, H. M. and Forsythe, I. D., 1995; Gan, L. and Kaczmarek, L.

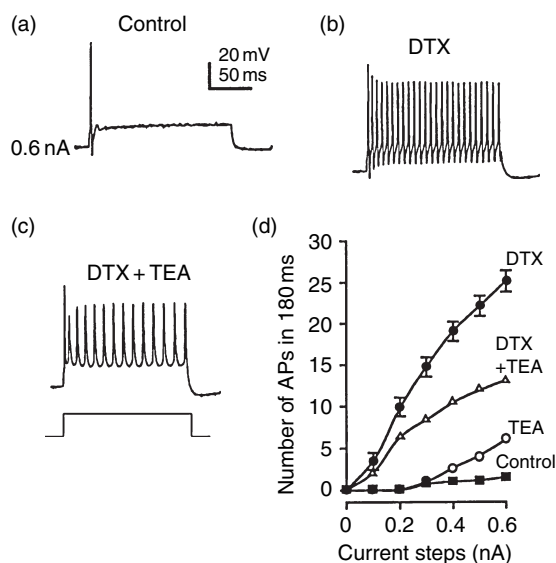


Figure 6 Potassium currents enhance signal processing in time-coding neurons. Shown are responses of MNTB neurons to current injections. (a) In the control condition, cells typically respond to depolarizing current steps with a single rapid action potential followed by a steady-state depolarization. The steady-state response is normally highly outward rectified (not shown). (b) When DTX, a Kv1 subunit specific blocker, is applied to the neuron, multiple spiking is evoked by the same current pulse. (c) Shows that by TEA application, high-threshold K^+ channels play an additional role in controlling membrane voltage. (d) Shows the firing rates across the population for the conditions in (a) through (c) and the TEA alone condition for two additional cells. Adapted from Brew, H. M. and Forsythe, I. D. 1995. Two voltage-dependent K^+ conductances with complementary functions in postsynaptic integration at a central auditory synapse. *J. Neurosci.* 15, 8011–8022. Change to the current values from original was made at the request of H. Brew.

K., 1998; Wang, L. Y. *et al.*, 1998). Several studies have shown that in the presence of low concentrations of tetraethylammonium chloride (TEA) which blocks K_{HT}^+ , cells fail to sustain the high-firing frequencies typically achieved by temporal coding neurons (Brew, H. M. and Forsythe, I. D., 1995; Wang, L. Y. *et al.*, 1998). Figure 6 shows that a TEA-sensitive conductance in MNTB cells contributes to the brevity of action potentials. Furthermore, recent studies suggest that K_{HT}^+ conductances can be modulated through phosphorylation in an activity-dependent manner (Macica, C. M. *et al.*, 2003; Song, P. *et al.*, 2005). This finding suggests the possibility that this conductance may be tuned to optimally preserve temporal fidelity over a large range of firing frequencies (Song, P. *et al.*, 2005).

The impact of K_{LVA}^+ conductances on phase-locking and modulation of firing frequency in NL was investigated by Reyes A. D. *et al.* (1996). Reyes and colleagues recorded evoked excitatory postsynaptic conductances (EPSCs) in NL, and then, based on these recordings, computed model input trains and injected the summed current into the cells through a patch pipette. This strategy allowed the experimenters to model variations in the size, number, and temporal properties of the inputs. They were able to show that as stimulus frequency increased, a reduction of the number and an increase in size of the inputs was necessary to maintain high firing rates and phase-locked discharges in NL cells. They demonstrated that NL neurons characteristically possess a large low-threshold potassium conductance and that this conductance was crucial for temporal coding. NL neurons in which this current was pharmacologically blocked or other brainstem neurons that did not possess this conductance, were unable to phase-lock to high input frequencies.

Work by Ohmori and colleagues investigated the tonotopic distribution of Kv1.1 type potassium channel subunits, which are often incorporated into voltage gated K^+ channels that underlie K_{LVA}^+ conductances. Using both physiological and immunohistochemical methods, they show that Kv1.1 subunits are not distributed evenly across the tonotopy of NL. NL cells in the mid- and high-frequency range appear to express Kv1.1 subunits and the associated conductance at higher levels than low-frequency neurons. Correlated with this effect is the observation that the middle-frequency NL neurons, the subset that physiologically had the strongest K_{LVA}^+ conductances, appear to have the smallest coincidence window. The authors suggested that these findings may explain behavioral data showing that sound localization is most precise in the middle-frequency range for many birds (Kuba, H. *et al.*, 2005).

An additional important observation from this series of studies was the demonstration that the input properties vary across the tonotopy such that low-frequency cells produce Excitatory post synaptic potentials (EPSPs) with a longer time course than their mid- and high-frequency counterparts. The long EPSP duration was attributable to dendritic filtering of low-frequency NL cells that results from the large surface area of dendrites (Rall, W., 1969; Koch, C. and Segev, I., 2000; Kuba, H. *et al.*, 2005). A possible consequence of this filtering property is that it may enhance the electrical isolation of dorsal and ventral dendrites and, thus, the inputs from either ear

from each other. This finding is significant because it is the first direct data to support the notion that the dendrite length gradient in NL is an adaptation for ITD processing of particular stimulus frequencies.

A fascinating assessment of the possible contribution of NL dendrites to ITD computation was made in an influential modeling study (Agmon-Snir, H. *et al.*, 1998). These authors proposed that the segregation of the ipsilateral and contralateral inputs to the dorsal and ventral dendrites, respectively, of NL neurons provides semi-isolated electrical compartments in which a series of inputs arriving near-simultaneously will add sublinearly within one electrical compartment. On the other hand, inputs arriving on separate dendrites will sum linearly in the soma. This mechanism could greatly enhance coincidence detection. Put simply, two inputs that arrive on separate dendrites and provide just enough current necessary to reach threshold would add sublinearly in a single dendrite and thus not generate a postsynaptic action potential. This mechanism would function to enhance a cell's responsiveness to binaural inputs, while suppressing the signaling of responses from coincident monaural input. The model also provided a rationale for the reduction of dendrite length with increasing frequency. Due to the amount of temporal error in phase-locking (or jitter), long dendrites, with longer duration membrane time constants, may expand their inputs in time and cause excess monaural summation at high frequencies where the stimulus period is brief, relative to the temporal jitter.

3.35.2.4 The Role of Inhibition in Nucleus Luminaris Function

The release of GABA in both NM and NL has unusual and important properties. GABA-receptor activation evokes a depolarizing response in these neurons. This property, first discovered by Hyson R. L. *et al.* (1995) in NL, is due to an unusually high internal Cl^- concentration. The reversal potential for the Cl^- conductance through $GABA_A$ receptors has been reported to be -25 and -37 mV by two separate studies using gramicidin perforated patch-clamp recording of NM cells (Lu, T. and Trussell, L. O., 2001; Monsivais, P. and Rubel, E. W., 2001). Depolarizing responses to GABA are not unusual at early stages of development in the auditory system or in other central neurons (Ben-Ari, Y. *et al.*, 1990; Cherubini, E. *et al.*, 1990; Kandler, K. and Friauf, E., 1995; Ehrlich, I. *et al.*, 1999; Kakazu, Y. *et al.*, 1999), but

are normally rapidly converted to hyperpolarizing responses. In mammalian auditory systems this generally occurs around the time of onset of hearing (Kandler, K. and Friauf, E., 1995; Smith, A. J. *et al.*, 2000; Magnusson, A. K. *et al.*, 2005). The precise mechanism underlying this shift is unknown, but is likely due to a change in Cl^- transporter expression (Kakazu, Y. *et al.*, 1999). In the chicken, depolarizing responses to GABA have been recorded well beyond hearing onset and appear to persist into maturity (Hackett, J. T. *et al.*, 1982; Jackson, H. *et al.*, 1982; Hyson, R. L. *et al.*, 1995; Yang, L. *et al.*, 1999; Monsivais, P. *et al.*, 2000; Lu, T. and Trussell, L. O., 2001).

What functional benefit is gained by this unusual property? In a series of studies from our laboratory, Monsivais and colleagues (Yang, L. *et al.*, 1999; Monsivais, P. *et al.*, 2000; Monsivais, P. and Rubel, E. W., 2001) showed that despite the depolarizing response to GABA, this input is generally inhibitory although occasional spiking from GABAergic input has been observed *in vitro* (Lu, T. and Trussell, L. O., 2001; Lu, Y. *et al.*, 2005). Indeed, Monsivais P. and Rubel E. W. (2001) showed that GABAergic depolarization into a superthreshold voltage range maintains its inhibitory function, and even exceeds the inhibitory potency that would derive from equal strength hyperpolarizing inputs. This depolarizing and potent inhibitory response is mediated through three cooperative mechanisms.

First, GABA release at NM or NL activates GABA_A channels generating a Cl^- conductance. High stimulation rates of inhibitory inputs to NM cause Ca^{2+} accumulation in GABAergic terminals resulting in a long-lasting postsynaptic plateau inhibition characterized by asynchronous release of GABA (Lu, T. and Trussell, L. O., 2000). The outward flux of Cl^- ions depolarizes the cell membrane activating strong K_{LVA}^+ conductances that dramatically lower the input resistance and thus provide a shunting inhibition for subsequent excitatory inputs. Finally, the slow and sustained GABA-induced depolarization causes inactivation of voltage gated Na^+ channels and, as a consequence, threshold shifts to depolarized values (Monsivais, P. and Rubel, E. W., 2001). Our recent study suggested that excessive GABA-evoked depolarization might be limited by GABA_B receptor activation on the GABAergic terminals. GABA_B receptor activation at these sites reduces the release of transmitter and subsequently generates less postsynaptic depolarization (Lu, Y. *et al.*, 2005).

Funabiki K. *et al.* (1998), in the Ohmori lab, tested the hypothesis that GABAergic input to NL improves coincidence detection as well. In an elegant series of experiments, they simulated binaural inputs by current injection or direct stimulation of NM axons and varied the interval between inputs to simulate a range of ITDs. They showed that during GABA application, the range of binaural intervals that evoked responses in the NL neurons (or response window) was reduced by 70%. This study clearly demonstrated GABA's potentially advantageous effect on the computational properties of NL.

To date, there have been no *in vivo* studies in birds to directly address the role of endogenous GABAergic input to the temporal coding nuclei. However, several studies have been done that underscore the potentially critical influence inhibition may have on ITD coding. Among the most important of these, Peña and colleagues in the Konishi lab published a pair of studies using loose-patch recording of NM and NL neurons providing superior isolation of responses. The NL recordings explored the stability of ITD tuning when neurons were challenged with a range of intensity changes to the two ears such that levels were shifted simultaneously in both ears (diotically) or differentially in each ear (dichotically) (Pena, J. L. *et al.*, 1996; Viète, S. *et al.*, 1997). Figure 7 shows that NL neurons possess a remarkable ability to maintain their best ITD (the ITD evoking the strongest response) and large firing-rate modulations with ITD over a large dynamic range of diotically presented intensity changes (Pena, J. L. *et al.*, 1996). Additionally, in the second paper, Viète S. *et al.* (1997) showed that for broadband stimuli, a neuron's best ITD remained fairly stable when the input intensity to either ear was unequal, suggesting that the system may include a mechanism to correct for differences in input strengths. These authors suggested that inhibition might provide the input necessary to preserve the stability of the ITD selective response under a broad range of conditions, although in their hands, evidence for such a mechanism was not forthcoming.

Our recent studies on the detailed anatomy of the GABAergic input to these nuclei from the SON led to predictions about a specific inhibitory mechanism for the observations noted earlier and further suggest that the inhibitory components of the ITD processing circuitry may have a fundamental role in ITD processing (Burger, R. M. *et al.*, 2005). In the chicken, most of the inhibitory input to the cochlear nuclei and NL is provided by the ipsilateral SON (Lachica,

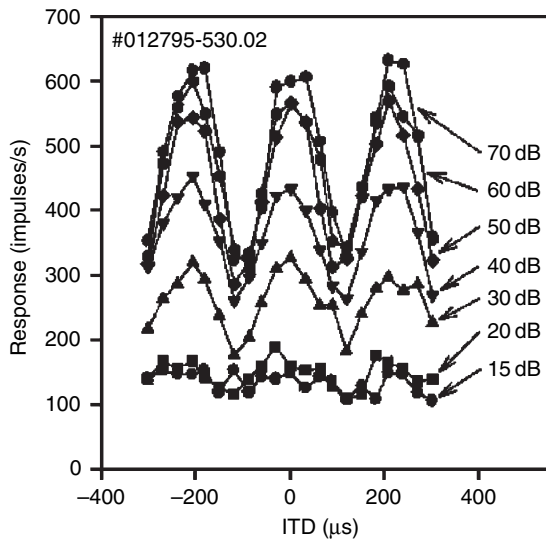


Figure 7 NL neurons possess a remarkable ability to maintain ITD selectivity over a broad dynamic range. In this figure, Pena and colleagues showed that NL neurons preserve their best ITD and a fairly large dynamic response over a large range of binaurally presented intensity changes. These data suggest that some mechanism, perhaps inhibition, may adjust the gain of the NL neuron's responses, allowing it to be selective at low intensities and preventing saturation at high intensities. Reproduced from Pena, J. L., Viète, S., Albeck, Y., and Konishi, M. 1996. Tolerance to sound intensity of binaural coincidence detection in the nucleus laminaris of the owl. *J. Neurosci.* 16, 7046–7054.

E. A. *et al.*, 1994; Westerberg, B. D. and Schwarz, D. W., 1995; Yang, L. *et al.*, 1999; Burger, R. M. *et al.*, 2005). The SON, in turn, receives its input from three sources, NA, NL, and the contralateral SON (Yang, L. *et al.*, 1999). The NA and NL input is glutamatergic and excitatory, and the contralateral SON input is likely to be inhibitory. Thus, the inhibitory circuitry of the avian auditory system is composed of a negative feedback loop on each side of the brainstem. In addition, these two feedback circuits appear to be negatively coupled to one another (Figure 8).

This anatomical arrangement provides clues as to how the system may work. We developed a conceptual model that suggested that this arrangement would provide a mechanism to preserve ITD encoding by equalizing the input strength to NL (Burger, R. M. *et al.*, 2005). A computational model went further in testing this hypothesis in a model avian auditory brainstem network using realistic biological parameters (Dasika, V. K. *et al.*, 2005).

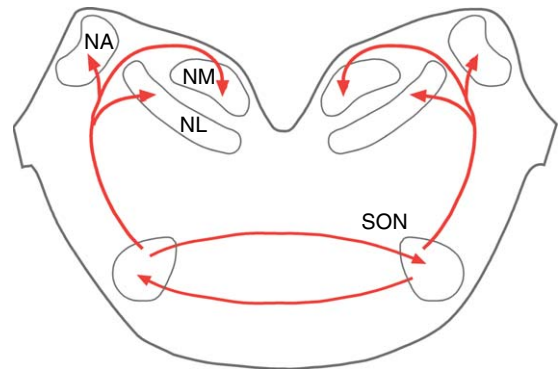


Figure 8 The inhibitory circuitry of the avian auditory brainstem. The majority of inhibitory input to the time-coding system emanates from the predominantly GABAergic SON. The SON which receives excitatory input from both NA and NL provides inhibition back to all ipsilateral brainstem nuclei forming an inhibitory feedback loop. These parallel feedback loops are coupled by the crossed reciprocal and putatively inhibitory connection between the SONs. These negatively coupled feedback circuits may be involved in offsetting bilateral differences in input strength to NL.

3.35.3 Interaural Time Disparity Processing in the Medial Superior Olive

The MSO in mammals receives a similar complement of inputs to that of NL in avians. However, important differences exist which raise interesting comparative questions as to the nature of ITD processing in MSO. In this section, we will first discuss the known anatomy and physiology of the MSO leading to some current issues in the field of ITD processing in the final section.

3.35.3.1 Mammalian Interaural Time Disparity-Encoding Circuitry

The MSO receives four principal inputs, one excitatory and one inhibitory, driven from each ear (Figure 9). The excitatory inputs derive bilaterally from the spherical bushy cells of the anteroventral cochlear nucleus (AVCN) where neurons specialized to faithfully transmit temporal aspects of the acoustic signal project to the MSO (Stotler, W. A., 1953; Glendinning, K. K. *et al.*, 1985; Cant, N. B. and Hyson, R. L., 1992; Smith, P. H. *et al.*, 1993). For a thorough review of superior olive anatomy see Thompson A. M. and Schofield B. R. (2000). MSO neurons, like their avian NL counterparts, have bipolar dendrites oriented roughly in the mediolateral plane, with each dendrite receiving input from

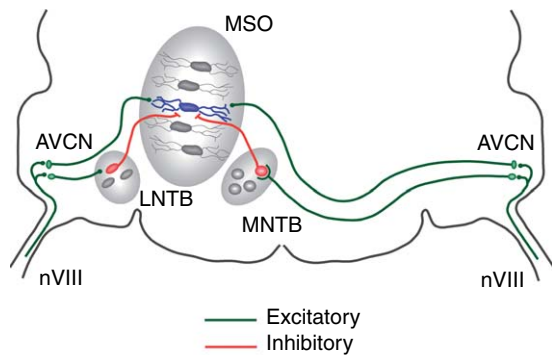


Figure 9 Input pathways to the MSO. The MSO receives excitatory input green pathways from both ears via bushy cells of the AVCN where nVIII inputs convey phase-locked discharges with large endbulb of Held synapses. Inhibition from both ears is also derived from input circuitry that is specialized to preserve temporal information. Input from the contralateral ear is conveyed via the glycinergic MNTB where bushy cell axons make large Caylx of Held synapses onto MNTB neuron somas. The ipsilateral inhibitory input is derived from the LNTB where enlarged synaptic endings from AVCN neurons appear to be specialized for temporal encoding.

its proximal ear (Figure 4) (Stotler, W. A., 1953; Smith, P. H. *et al.*, 1993).

The inhibitory input from the contralateral ear is derived from the medial nucleus of the trapezoid body (MNTB) (Kuwabara, N. and Zook, J. M., 1992; Smith, P. H. *et al.*, 1998). The glycinergic MNTB receives input from the anteroventral cochlear nucleus (AVCN) through large caliciform synapses that convert the precisely timed excitatory input into a precisely timed inhibitory output. The ipsilateral inhibition to the MSO is derived from the lateral nucleus of the trapezoid body (LNTB) where similar large synapses from AVCN bushy cells drive its glycinergic inhibitory output (Cant, N. B. and Hyson, R. L., 1992; Kuwabara, N. and Zook, J. M., 1992; Spirou, G. A. *et al.*, 1998).

A fundamental component of ITD-encoding circuitry according to the Jeffress hypothesis is an orderly series of input delay lines. In birds, NM input to the contralateral NL exhibits a clear anatomical axon length gradient that corresponds to the orderly representation of interaural phase delays. The evidence for delay lines in mammals is controversial. In the cat MSO, some compelling data suggests that the input axons from the contralateral ear may be arranged to generate delay lines, such that the rostral MSO cells receive the shortest length input collateral and the caudal cells receive the longest

(Smith, P. H. *et al.*, 1993; Beckius, G. E. *et al.*, 1999). This anatomical arrangement agrees fairly well with the physiologically observed rough topography of ITD representation reported in the cat (Yin, T. C. and Chan, J. C., 1990). However, data from both anatomical studies shows that many input axons innervate only small segments of the MSO and not the entire extent of the nucleus as they do in NL. In addition, there have not been similar systematic physiological studies of the inputs to MSO at the level of those in NL (Sullivan, W. E. and Konishi, M., 1986; Carr, C. E. and Konishi, M., 1990; Overholt, E. M. *et al.*, 1992; Joseph, A. W. and Hyson, R. L., 1993) to confirm the presence of functional delay lines as a general feature in mammals.

3.35.3.2 Response Properties of Medial Superior Olive Neurons

The classic work of Goldberg J. M. and Brown P. B. (1969) was the first thorough study of the MSO role in ITD processing. Goldberg and Brown showed that MSO neurons in the dog were: (1) excited by input to both ears, (2) phase-locked to the stimulus waveform, and (3) optimally driven by binaural input with a particular delay that could be predicted based on the ITD required for the coincidence of monaural delays from each ear. They also observed several features of MSO neural responses that they attributed to inhibition, such as frequency selectivity, nonmonotonic input/output functions when driven by sound to one or both ears, and binaural firing rates that fell below the firing rate to either ear alone at the worst ITD (the ITD evoking the lowest firing rate).

The presence of brainstem neurons that process ITDs in a similar fashion to those observed in the dog have been documented in the cat, rabbit, gerbil, and kangaroo rat (Moushegian, G. *et al.*, 1967; Moushegian, G. *et al.*, 1975; Yin, T. C. and Chan, J. C., 1990; Spitzer, M. W. and Semple, M. N., 1995; Batra, R. and Fitzpatrick, D. C., 1997; Batra, R. *et al.*, 1997a; 1997b). In most of these studies the dominant class of MSO neurons exhibited evidence of phase-locked excitatory input from each ear and responded selectively to ITD selectivity to varying binaural stimuli. This suggests that most MSO neurons derive their response properties by cross-correlation of the phase-locked excitation from each ear.

A series of studies from Batra and colleagues (Batra, R. and Fitzpatrick, D. C., 1997; Batra, R. *et al.*, 1997a; 1997b) investigated ITD processing in the superior olivary complex. An important finding

of these studies was that coincidence of excitation from one ear and inhibition from the opposite ear also can impart ITD sensitivity on a neuron. Such neurons were referred to as troughers, following the nomenclature of Kuwada S. and Yin T. C. (1983) and Yin T. C. and Kuwada S. (1983a; 1983b), and were also observed in earlier studies of the LSO (Finlayson, P. G. and Caspary, D. M., 1991; Joris, P. X. and Yin, T. C., 1995). Spiking in trougher neurons is suppressed at a particular ITD regardless of stimulus frequency. Thus, these neurons are inactivated by coincidence of their inputs. However, it remains inconclusive whether or not this class of neurons resides within the MSO proper, but rather, may be the predominant ITD selective cell type in the neighboring lateral superior olive.

3.35.3.3 Intrinsic Properties of Medial Superior Olive Neurons

MSO neurons share several morphological and physiological properties with NL cells. Similar to other neurons that are specialized for processing temporal information (as cited earlier), injection of depolarizing current into principal MSO cells typically results in a single action potential followed by a sustained depolarization (Smith, P. H., 1995). The sustained portion of the response shows strong outward rectification. Application of 4-AP increases the number of action potentials and reduces the degree of rectification. This suggests that the large K^+ _{LVA} type currents dominate the intrinsic membrane voltage responses in MSO neurons (Smith, P. H., 1995).

A study utilizing both physiological and modeling methods tested the role of K^+ _{LVA} in signal detection in the presence of noisy inputs. Using a similar approach to that used by Reyes A. D. *et al.* (1996) in NL, Svirskis G. *et al.* (2002) injected subthreshold simulated excitatory postsynaptic conductances (EPSPs) as signals in a background of noisy subthreshold currents into normal and dendrotoxin (DTX)-treated MSO cells. DTX is a specific blocker of Kv1 family subunit containing channels (Robertson, B. *et al.*, 1996). They used a spike-triggered reverse correlation paradigm to determine the optimal current waveform to evoke spiking and found that control cells required very rapid inward currents, indicating a brief integration window. In DTX-treated cells the integration window was broader and the phase-locking to simulated EPSPs was poor. Thus, NL and MSO possess similar intrinsic mechanisms to enhance ITD selectivity.

In a later paper Svirskis G. *et al.* (2004) showed that at rest, many voltage-gated Na^+ channels are inactivated in MSO cells. Spike-triggered reverse correlations showed that MSO neurons fired optimally following a brief hyperpolarizing current. Manipulations of the Na^+ current showed that brief hyperpolarizing inputs have a role in releasing Na^+ channels from inactivation, thereby increasing the spike probability for a subsequent depolarizing input. Thus, the Na^+ channel properties in MSO cells may interact with inhibitory inputs to shape the coincidence window.

3.35.3.4 The Role of Inhibition in the Medial Superior Olive

Speculation on the contribution of inhibition in MSO responses has persisted in the literature since Goldberg J. M. and Brown P. B. (1969) noted that the firing rate to binaural stimuli that were at the worst ITD were below the rates evoked by stimulation of either ear alone. Similar observations have been noted in subsequent studies (Yin, T. C. and Chan, J. C., 1990; Spitzer, M. W. and Semple, M. N., 1995; 1998). Abundant anatomical evidence shows direct innervation of the MSO by both the glycinergic MNTB and the LNTB (Cant, N. B. and Hyson, R. L., 1992; Kuwabara, N. and Zook, J. M., 1992; Smith, P. H. *et al.*, 1998).

Investigation of these inputs has been made in slice preparations of both gerbil and rat (Grothe, B. and Sanes, D. H., 1993; 1994; Smith, A. J. *et al.*, 2000; Magnusson, A. K. *et al.*, 2005). Grothe B. and Sanes D. H. (1994) showed that glycinergic input suppressed firing of MSO cells *in vitro* at particular stimulus intervals between shocks to ipsilateral and contralateral inputs. Studies by Smith A. J. *et al.* (2000) in the rat and Magnusson A. K. *et al.* (2005) in the gerbil investigated the development of inhibitory input to the MSO and showed that between the early postnatal period and the week following the onset of hearing, inhibitory inputs to MSO switch from slow depolarizing and predominantly GABAergic to relatively fast, hyperpolarizing, and predominantly glycinergic inputs. A similar developmental pattern has been described in the neighboring lateral superior olive (LSO), which receives collateral MNTB input (Kandler, K. and Friauf, E., 1995; Kotak, V. C. *et al.*, 1998; Nabekura, J. *et al.*, 2004; Magnusson, A. K. *et al.*, 2005). In the LSO the developmental conversion of inhibitory inputs represents a gradual switch from GABA to glycine transmitter expression within individual inhibitory terminals rather than a replacement

of GABAergic input axons by glycinergic ones (Nabekura, J. *et al.*, 2004).

The first study to test the role of inhibition in MSO coding *in vivo* by manipulating the glycinergic receptor activation yielded striking results. These results suggest a critical difference between avian and mammalian strategies for computation of ITDs. Brand A. *et al.* (2002) recorded from the gerbil MSO using multibarrel microelectrodes that allowed them to block the glycinergic input to MSO neurons with strychnine during recordings. Their data revealed that in the presence of strychnine, all MSO neurons had maximal responses at ITD values near 0 μ s (Figure 10). In control recordings, on the other hand, most neurons had a best ITD favoring sounds leading in the contralateral ear and outside the physiological range (the maximum range of ITD experienced by the animal under normal conditions). These data suggest that ITD processing in the gerbil may not rely on delays imposed on MSO by input axons but rather, the inhibitory inputs provided by the MNTB and/or the LNTB shape the selectivity.

Brand A. *et al.* (2002) supported their conclusions with computational modeling that showed that interaction between very rapid glycinergic inputs and the glutamatergic AVCN inputs is sufficient to generate the normal ITD responses. Since inhibitory inputs possessing such rapid kinetics have not been observed in intracellular studies of MSO neurons (Smith, A. J. *et al.*, 2000; Magnusson, A. K. *et al.*, 2005), further studies will be required to resolve exactly how inhibition imparts its apparently critical contribution to MSO response properties.

3.35.3.5 The Neural Code for Interaural Time Disparity in Mammals

A second important finding of the Brand A. *et al.* (2002) study is that the peaks of the ITD functions in the control condition almost always occurred outside of the physiological range of ITDs. Similar results have been observed in the gerbil DNLL and the guinea pig inferior colliculus (McAlpine, D. *et al.*, 2001; Seidl, A. H. and Grothe, B., 2005). These organisms share the characteristics of having both, low-frequency hearing and small heads. As a consequence, the role of inhibition identified in the gerbil raises considerable doubt regarding the notion that ITD processing is simply a function of coincidence of binaural excitatory delays.

The recent progress discussed earlier has compelled researchers in the field to re-evaluate the nature of ITD representation in the mammalian

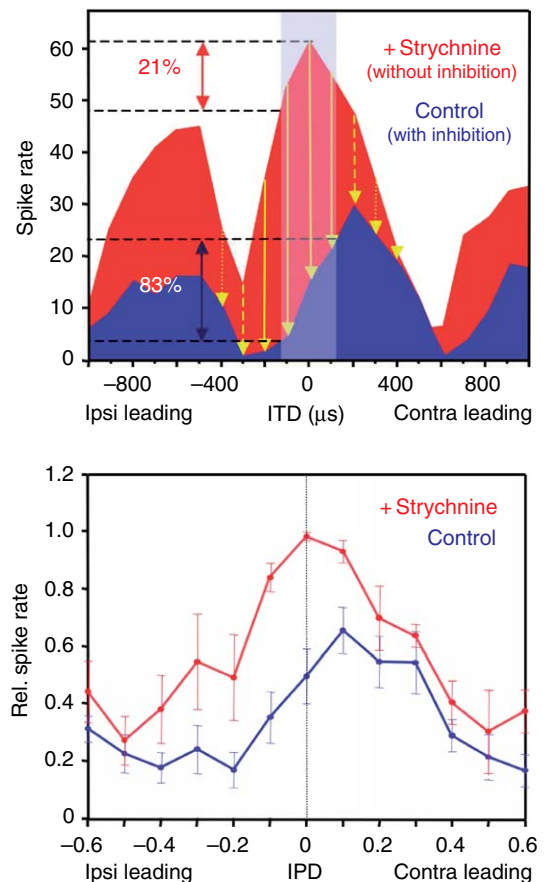


Figure 10 Inhibition shapes ITD functions in MSO. The top panel shows the ITD response functions of an MSO neuron before blue function and after red function application of strychnine, a glycine-receptor antagonist. The control condition data indicate that the peak response falls outside the range of naturally occurring ITDs shaded area but that the steepest slope of the function falls across zero ITD. When strychnine was applied, the neuron shifted its best ITD to near-zero, and had a rather small dynamic response within the physiological range. In the lower panel, the population data suggests that a primary consequence of inhibition in the MSO is to shift the location of the peak (or the slope) of ITD functions toward ITDs that lead in the contralateral ear. Reproduced from Macmillan Publishers LTD: Nature, from the study by Brand, A., Behrend, O., Marquardt, T., McAlpine, D., and Grothe, B. 2002. Precise inhibition is essential for microsecond interaural time difference coding. *Nature* 417, 543–547.

nervous system. This topic has been thoroughly and clearly discussed elsewhere (Grothe, B., 2003; McAlpine, D. and Grothe, B., 2003) and the arguments will not be recounted here, but the discussion rests on two possible, and not mutually exclusive, strategies of ITD representation in the nervous system.

The first possible coding strategy can be likened to a labeled line paradigm and is derived from the Jeffress model. In this scheme a neuron will have a peak response at a particular ITD within the physiological range of ITDs. Across the population of coding neurons (i.e., MSO, NL) all spatial positions (ITDs) will be represented by different subsets of neurons according to where their peak sensitivity lies within auditory space. The second strategy depends on comparing population responses, between two broadly tuned spatial channels (McAlpine, D. *et al.*, 2001; Palmer, A. R., 2004). In this scheme, information on the sound source location would depend not on the firing rate of particular neurons sensitive to small regions of space, but on a comparison of activity between the two MSOs. Each MSO neuron would respond to many positions in space, but in a graded way such that sound sources in the ipsilateral hemifield will evoke little activity while sound sources in the contralateral hemifield will evoke strong responses. Under this scheme sound source position is resolved only after a higher-order comparison of activity from the two MSOs.

The relative utility of these two coding schemes depends on the physical relationships between the stimulus frequency (wavelength) and the animal's head size. At the extremes, a low-frequency sound for an animal with a small head, the range of available IPDs is relatively small; thus broad population coding may be optimal. For higher frequencies and for animals with wide heads, there is an ample range of IPDs for which neurons could be constructed to be differentially sensitive. A recent modeling study took into account the relationships between stimulus frequency, interaural phase, and head size for four animals with different hearing ranges and head sizes (Harper, N. S. and McAlpine, D., 2004). The authors showed that across the tonotopic range for each animal, one or a combination of both coding strategies may be optimal depending on the stimulus frequency.

3.35.4 Summary and Conclusion

In both birds and mammals elegant circuitry has evolved to compute sound source location. The circuits devoted to low-frequency processing involving NL and MSO share many features designed to preserve or enhance extraction of temporal information from nVIII inputs. These include both morphological and intrinsic membrane specializations throughout the circuitry that are remarkably similar across these vertebrate classes. That being said, two systems

appear to differ in several ways that are still under investigation. These include the presence or absence of delay lines, the nature of the ITD code, as well as the role of inhibitory components of each system.

A suite of studies spanning the last two decades in both birds and mammals has elucidated the importance of inhibitory circuitry for ITD processing. The mammalian studies have demonstrated that MSO neurons receive a rapid and glycinergic hyperpolarizing inhibition from auditory pathways specialized to process temporal information from each ear. In contrast, avian ITD-processing neurons in NL receive a depolarizing slow GABAergic input that is derived from an auditory center that appears not to preserve phase-locked timing information with both monaural and binaural responses. In mammals, the limited data available suggest that a temporally constrained inhibitory input is a crucial factor in setting ITD selectivity in the MSO, but at this time a well-supported model for how the inhibition imparts selectivity on these cells is lacking. In birds, the slow inhibitory input seems to be involved in both enhancing the intrinsic membrane properties of time-coding neurons and perhaps binaurally controlling the system gain. The contrasting nature of inhibition in these systems represents one of the most fundamental differences between avian and mammalian circuits for processing ITDs. A clear understanding of inhibitory function in both NL and MSO will be critical to resolving the nature of ITD encoding at these primary sites of binaural computation.

Acknowledgments

We thank Mark Konishi, Helen Brew, Benedikt Grothe, the Society for Neuroscience, and Nature Publishing Group for permission to present their figures in our review. Finally, we thank Staci Sorensen, Olga Alexandrova, and Michael Pecka for contributions of images used in this chapter.

References

- Adamson, C. L., Reid, M. A., Mo, Z. L., Bowne-English, J., and Davis, R. L. 2002. Firing features and potassium channel content of murine spiral ganglion neurons vary with cochlear location. *J. Comp. Neurol.* 447, 331–350.
- Agmon-Snir, H., Carr, C. E., and Rinzel, J. 1998. The role of dendrites in auditory coincidence detection. *Nature* 393, 268–272.

- Bal, R. and Oertel, D. 2001. Potassium currents in octopus cells of the mammalian cochlear nucleus. *J. Neurophysiol.* 86, 2299–2311.
- Banks, M. I. and Smith, P. H. 1992. Intracellular recordings from neurobiotin-labeled cells in brain slices of the rat medial nucleus of the trapezoid body. *J. Neurosci.* 12, 2819–2837.
- Batra, R. and Fitzpatrick, D. C. 1997. Neurons sensitive to interaural temporal disparities in the medial part of the ventral nucleus of the lateral lemniscus. *J. Neurophysiol.* 78, 511–515.
- Batra, R., Kuwada, S., and Fitzpatrick, D. C. 1997a. Sensitivity to interaural temporal disparities of low- and high-frequency neurons in the superior olivary complex. II. Coincidence detection. *J. Neurophysiol.* 78, 1237–1247.
- Batra, R., Kuwada, S., and Fitzpatrick, D. C. 1997b. Sensitivity to interaural temporal disparities of low- and high-frequency neurons in the superior olivary complex. I. Heterogeneity of responses. *J. Neurophysiol.* 78, 1222–1236.
- Beckius, G. E., Batra, R., and Oliver, D. L. 1999. Axons from anteroventral cochlear nucleus that terminate in medial superior olive of cat: observations related to delay lines. *J. Neurosci.* 19, 3146–3161.
- Ben-Ari, Y., Rovira, C., Gaiarsa, J. L., Corradetti, R., Robain, O., and Cherubini, E. 1990. GABAergic mechanisms in the CA3 hippocampal region during early postnatal life. *Prog. Brain Res.* 83, 313–321.
- Brand, A., Behrend, O., Marquardt, T., McAlpine, D., and Grothe, B. 2002. Precise inhibition is essential for microsecond interaural time difference coding. *Nature* 417, 543–547.
- Brew, H. M. and Forsythe, I. D. 1995. Two voltage-dependent K^+ conductances with complementary functions in postsynaptic integration at a central auditory synapse. *J. Neurosci.* 15, 8011–8022.
- Burger, R. M., Cramer, K. S., Pfeiffer, J. D., and Rubel, E. W. 2005. Avian superior olivary nucleus provides divergent inhibitory input to parallel auditory pathways. *J. Comp. Neurol.* 481, 6–18.
- Cant, N. B. and Hyson, R. L. 1992. Projections from the lateral nucleus of the trapezoid body to the medial superior olivary nucleus in the gerbil. *Hear. Res.* 58, 26–34.
- Carney, L. H. 1992. Modelling the sensitivity of cells in the anteroventral cochlear nucleus to spatiotemporal discharge patterns. *Philos. Trans. R. Soc. Lond. B. Biol. Sci.* 336, 403–406.
- Carr, C. E. and Boudreau, R. E. 1996. Development of the time coding pathways in the auditory brainstem of the barn owl. *J. Comp. Neurol.* 373, 467–483.
- Carr, C. E. and Code, R. A. 2000. Anatomy and Physiology of the Central Auditory System of Birds and Reptiles. In: *Comparative Hearing: Birds and Reptiles* (eds. A. N. Popper, R. R. Fay, and R. J. Dooling), pp. 197–248. Springer.
- Carr, C. E. and Konishi, M. 1990. A circuit for detection of interaural time differences in the brain stem of the barn owl. *J. Neurosci.* 10, 3227–3246.
- Carr, C. E. and Soares, D. 2002. Evolutionary convergence and shared computational principles in the auditory system. *Brain. Behav. Evol.* 59, 294–311.
- Carr, C. E., Fujita, I., and Konishi, M. 1989. Distribution of GABAergic neurons and terminals in the auditory system of the barn owl. *J. Comp. Neurol.* 286, 190–207.
- Carr, C. E., Soares, D., Parameshwaran, S., and Perney, T. 2001. Evolution and development of time coding systems. *Curr. Opin. Neurobiol.* 11, 727–733.
- Cherubini, E., Rovira, C., Gaiarsa, J. L., Corradetti, R., and Ben Ari, Y. 1990. GABA mediated excitation in immature rat CA3 hippocampal neurons. *Int. J. Dev. Neurosci.* 8, 481–490.
- Code, R. A., Burd, G. D., and Rubel, E. W. 1989. Development of GABA immunoreactivity in brainstem auditory nuclei of the chick: ontogeny of gradients in terminal staining. *J. Comp. Neurol.* 284, 504–518.
- Colburn, H. S. and Durlach, N. I. 1978. Models of Binaural Interaction. In: *Handbook of Perception* (eds. E. C. Carterette, and M. Friedman), pp. 467–518. Academic Press.
- Dasika, V. K., White, J. A., Carney, L. H., and Colburn, H. S. 2005. Effects of inhibitory feedback in a network model of avian brain stem. *J. Neurophysiol.* 94, 400–414.
- Ehrlich, I., Lohrke, S., and Friauf, E. 1999. Shift from depolarizing to hyperpolarizing glycine action in rat auditory neurones is due to age-dependent Cl^- regulation. *J. Physiol.* 520(Pt 1), 121–137.
- Finlayson, P. G. and Caspary, D. M. 1991. Low-frequency neurons in the lateral superior olive exhibit phase-sensitive binaural inhibition. *J. Neurophysiol.* 65, 598–605.
- Funabiki, K., Koyano, K., and Ohmori, H. 1998. The role of GABAergic inputs for coincidence detection in the neurones of nucleus laminaris of the chick. *J. Physiol.* 508(Pt 3), 851–869.
- Gan, L. and Kaczmarek, L. K. 1998. When, where, and how much? Expression of the $Kv3.1$ potassium channel in high-frequency firing neurons. *J. Neurobiol.* 37, 69–79.
- Glendenning, K. K., Hutson, K. A., Nudo, R. J., and Masterton, R. B. 1985. Acoustic chiasm II: anatomical basis of binaurality in lateral superior olive of cat. *J. Comp. Neurol.* 232, 261–285.
- Goldberg, J. M. and Brown, P. B. 1969. Response of binaural neurons of dog superior olivary complex to dichotic tonal stimuli: some physiological mechanisms of sound localization. *J. Neurophysiol.* 32, 613–636.
- Grigg, J. J., Brew, H. M., and Tempel, B. L. 2000. Differential expression of voltage-gated potassium channel genes in auditory nuclei of the mouse brainstem. *Hear. Res.* 140, 77–90.
- Grothe, B. 2003. New roles for synaptic inhibition in sound localization. *Nat. Rev. Neurosci.* 4, 540–550.
- Grothe, B. and Sanes, D. H. 1993. Bilateral inhibition by glycinergic afferents in the medial superior olive. *J. Neurophysiol.* 69, 1192–1196.
- Grothe, B. and Sanes, D. H. 1994. Synaptic inhibition influences the temporal coding properties of medial superior olivary neurons: an *in vitro* study. *J. Neurosci.* 14, 1701–1709.
- Hackett, J. T., Jackson, H., and Rubel, E. W. 1982. Synaptic excitation of the second and third order auditory neurons in the avian brain stem. *Neuroscience* 7, 1455–1469.
- Hall, J. L., 2nd 1965. Binaural interaction in the accessory superior-olivary nucleus of the cat. *J. Acoust. Soc. Am.* 37, 814–823.
- Harper, N. S. and McAlpine, D. 2004. Optimal neural population coding of an auditory spatial cue. *Nature* 430, 682–686.
- Hoy, R. R. and Robert, D. 1996. Tympanal hearing in insects. *Annu. Rev. Entomol.* 41, 433–450.
- Hyson, R. L., Reyes, A. D., and Rubel, E. W. 1995. A depolarizing inhibitory response to GABA in brainstem auditory neurons of the chick. *Brain Res.* 677, 117–126.
- Jackson, H., Hackett, J. T., and Rubel, E. W. 1982. Organization and development of brain stem auditory nuclei in the chick: ontogeny of postsynaptic responses. *J. Comp. Neurol.* 210, 80–86.
- Jeffress, L. A. 1948. A place theory of sound localization. *J. Comp. Physiol. Psychol.* 41, 35–39.
- Joris, P. X. and Yin, T. C. 1995. Envelope coding in the lateral superior olive. I. Sensitivity to interaural time differences. *J. Neurophysiol.* 73, 1043–1062.
- Joseph, A. W. and Hyson, R. L. 1993. Coincidence detection by binaural neurons in the chick brain stem. *J. Neurophysiol.* 69, 1197–1211.
- Kakazu, Y., Akaike, N., Komiyama, S., and Nabekura, J. 1999. Regulation of intracellular chloride by cotransporters in

- developing lateral superior olive neurons. *J. Neurosci.* 19, 2843–2851.
- Kandler, K. and Friauf, E. 1995. Development of glycinergic and glutamatergic synaptic transmission in the auditory brainstem of perinatal rats. *J. Neurosci.* 15, 6890–6904.
- Knudsen, E. I. and Konishi, M. 1979. Mechanisms of sound localization in the barn owl (*Tyto alba*). *J. Comp. Physiol. A Neuroethol. Sens. Neural. Behav. Physiol.* 133, 13–21.
- Koch, C. and Segev, I. 2000. The role of single neurons in information processing. *Nat. Neurosci.* 3(Suppl), 1171–1177.
- Kotak, V. C., Korada, S., Schwartz, I. R., and Sanes, D. H. 1998. A developmental shift from GABAergic to glycinergic transmission in the central auditory system. *J. Neurosci.* 18, 4646–4655.
- Kuba, H., Yamada, R., Fukui, I., and Ohmori, H. 2005. Tonotopic specialization of auditory coincidence detection in nucleus laminaris of the chick. *J. Neurosci.* 25, 1924–1934.
- Kubke, M. F., Massoglia, D. P., and Carr, C. E. 2002. Developmental changes underlying the formation of the specialized time coding circuits in barn owls (*Tyto alba*). *J. Neurosci.* 22, 7671–7679.
- Kuwabara, N. and Zook, J. M. 1992. Projections to the medial superior olive from the medial and lateral nuclei of the trapezoid body in rodents and bats. *J. Comp. Neurol.* 324, 522–538.
- Kuwada, S. and Yin, T. C. 1983. Binaural interaction in low-frequency neurons in inferior colliculus of the cat. I. Effects of long interaural delays, intensity, and repetition rate on interaural delay function. *J. Neurophysiol.* 50, 981–999.
- Lachica, E. A., Rubsamen, R., and Rubel, E. W. 1994. GABAergic terminals in nucleus magnocellularis and laminaris originate from the superior olivary nucleus. *J. Comp. Neurol.* 348, 403–418.
- Lu, T. and Trussell, L. O. 2000. Inhibitory transmission mediated by asynchronous transmitter release. *Neuron* 26, 683–694.
- Lu, T. and Trussell, L. O. 2001. Mixed excitatory and inhibitory GABA-mediated transmission in chick cochlear nucleus. *J. Physiol.* 535, 125–131.
- Lu, Y., Burger, R. M., and Rubel, E. W. 2005. GABA(B) receptor activation modulates GABA(A) receptor-mediated inhibition in chicken nucleus magnocellularis neurons. *J. Neurophysiol.* 93, 1429–1438.
- Lu, Y., Monsivais, P., Tempel, B. L., and Rubel, E. W. 2004. Activity-dependent regulation of the potassium channel subunits Kv1.1 and Kv3.1. *J. Comp. Neurol.* 470, 93–106.
- Macica, C. M., von Hehn, C. A., and Wang, L. Y., *et al.* 2003. Modulation of the kv3.1b potassium channel isoform adjusts the fidelity of the firing pattern of auditory neurons. *J. Neurosci.* 23, 1133–1141.
- Magnusson, A. K., Kapfer, C., Grothe, B., and Koch, U. 2005. Maturation of Glycinergic Inhibition in the Gerbil Medial Superior Olive after Hearing Onset. *J. Physiol.* 568, 497–512.
- Maki, K. and Furukawa, S. 2005. Acoustical cues for sound localization by the Mongolian gerbil, *Meriones unguiculatus*. *J. Acoust. Soc. Am.* 118, 872–886.
- Manis, P. B. and Marx, S. O. 1991. Outward currents in isolated ventral cochlear nucleus neurons. *J. Neurosci.* 11, 2865–2880.
- McAlpine, D. and Grothe, B. 2003. Sound localization and delay lines – do mammals fit the model? *Trends Neurosci.* 26, 347–350.
- McAlpine, D., Jiang, D., and Palmer, A. R. 2001. A neural code for low-frequency sound localization in mammals. *Nat. Neurosci.* 4, 396–401.
- Monsivais, P. and Rubel, E. W. 2001. Accommodation enhances depolarizing inhibition in central neurons. *J. Neurosci.* 21, 7823–7830.
- Monsivais, P., Yang, L., and Rubel, E. W. 2000. GABAergic inhibition in nucleus magnocellularis: implications for phase locking in the avian auditory brainstem. *J. Neurosci.* 20, 2954–2963.
- Moushegian, G., Rupert, A. L., and Langford, T. L. 1967. Stimulus coding by medial superior olivary neurons. *J. Neurophysiol.* 30, 1239–1261.
- Moushegian, G., Rupert, A. L., and Gidda, J. S. 1975. Functional characteristics of superior olivary neurons to binaural stimuli. *J. Neurophysiol.* 38, 1037–1048.
- Nabekura, J., Katsurabayashi, S., Kakazu, Y., *et al.* 2004. Developmental switch from GABA to glycine release in single central synaptic terminals. *Nat. Neurosci.* 7, 17–23.
- Oertel, D. 1983. Synaptic responses and electrical properties of cells in brain slices of the mouse anteroventral cochlear nucleus. *J. Neurosci.* 3, 2043–2053.
- Oertel, D. 1997. Encoding of timing in the brain stem auditory nuclei of vertebrates. *Neuron* 19, 959–962.
- Overholt, E. M., Rubel, E. W., and Hyson, R. L. 1992. A circuit for coding interaural time differences in the chick brainstem. *J. Neurosci.* 12, 1698–1708.
- Palmer, A. R. 2004. Reassessing mechanisms of low-frequency sound localisation. *Curr. Opin. Neurobiol.* 14, 457–460.
- Parameshwaran, S., Carr, C. E., and Perney, T. M. 2001. Expression of the Kv3.1 potassium channel in the avian auditory brainstem. *J. Neurosci.* 21, 485–494.
- Parameshwaran-Iyer, S., Carr, C. E., and Perney, T. M. 2003. Localization of KCNC1 (Kv3.1) potassium channel subunits in the avian auditory nucleus magnocellularis and nucleus laminaris during development. *J. Neurobiol.* 55, 165–178.
- Parks, T. N. and Rubel, E. W. 1975. Organization and development of brain stem auditory nuclei of the chicken: organization of projections from n. magnocellularis to n. laminaris. *J. Comp. Neurol.* 164, 435–448.
- Pena, J. L., Viète, S., Albeck, Y., and Konishi, M. 1996. Tolerance to sound intensity of binaural coincidence detection in the nucleus laminaris of the owl. *J. Neurosci.* 16, 7046–7054.
- Perney, T. M. and Kaczmarek, L. K. 1997. Localization of a high threshold potassium channel in the rat cochlear nucleus. *J. Comp. Neurol.* 386, 178–202.
- Perney, T. M., Marshall, J., Martin, K. A., Hockfield, S., and Kaczmarek, L. K. 1992. Expression of the mRNAs for the Kv3.1 potassium channel gene in the adult and developing rat brain. *J. Neurophysiol.* 68, 756–766.
- Pollak, G. D., Burger, R. M., and Klug, A. 2003. Dissecting the circuitry of the auditory system. *Trends Neurosci.* 26, 33–39.
- Pollak, G. D., Burger, R. M., Park, T. J., Klug, A., and Bauer, E. E. 2002. Roles of inhibition for transforming binaural properties in the brainstem auditory system. *Hear. Res.* 168, 60–78.
- Rall, W. 1969. Time constants and electrotonic length of membrane cylinders and neurons. *Biophys. J.* 9, 1483–1508.
- Rathouz, M. and Trussell, L. 1998. Characterization of outward currents in neurons of the avian nucleus magnocellularis. *J. Neurophysiol.* 80, 2824–2835.
- Rayleigh, L. S. 1907. On our perception of sound direction. *Philos. Mag.* 13, 214–232.
- Reyes, A. D., Rubel, E. W., and Spain, W. J. 1994. Membrane properties underlying the firing of neurons in the avian cochlear nucleus. *J. Neurosci.* 14, 5352–5364.
- Reyes, A. D., Rubel, E. W., and Spain, W. J. 1996. *In vitro* analysis of optimal stimuli for phase-locking and time-delayed modulation of firing in avian nucleus laminaris neurons. *J. Neurosci.* 16, 993–1007.
- Robert, D., Miles, R. N., and Hoy, R. R. 1996. Directional hearing by mechanical coupling in the parasitoid fly *Ormia ochracea*. *J. Comp. Physiol. A* 179, 29–44.
- Robertson, B., Owen, D., Stow, J., Butler, C., and Newland, C. 1996. Novel effects of dendrotoxin homologues on subtypes

- of mammalian Kv1 potassium channels expressed in *Xenopus* oocytes. *FEBS Lett.* 383, 26–30.
- Rothman, J. S., Young, E. D., and Manis, P. B. 1993. Convergence of auditory nerve fibers onto bushy cells in the ventral cochlear nucleus: implications of a computational model. *J. Neurophysiol.* 70, 2562–2583.
- Rubel, E. W. and Parks, T. N. 1975. Organization and development of brain stem auditory nuclei of the chicken: tonotopic organization of n. magno-cellularis and n. laminaris. *J. Comp. Neurol.* 164, 411–433.
- Rudy, B. and McBain, C. J. 2001. Kv3 channels: voltage-gated K⁺ channels designed for high-frequency repetitive firing. *Trends Neurosci.* 24, 517–526.
- Scott, L. L., Mathews, P. J., and Golding, N. L. 2005. Posthearing developmental refinement of temporal processing in principal neurons of the medial superior olive. *J. Neurosci.* 25, 7887–7895.
- Seidl, A. H. and Grothe, B. 2005. Development of sound localization mechanisms in the Mongolian Gerbil is shaped by early acoustic experience. *J. Neurophysiol.* 94, 1028–1036.
- Smith, A. J., Owens, S., and Forsythe, I. D. 2000. Characterisation of inhibitory and excitatory postsynaptic currents of the rat medial superior olive. *J. Physiol.* 529(Pt 3), 681–698.
- Smith, D. J. and Rubel, E. W. 1979. Organization and development of brain stem auditory nuclei of the chicken: dendritic gradients in nucleus laminaris. *J. Comp. Neurol.* 186, 213–239.
- Smith, P. H. 1995. Structural and functional differences distinguish principal from nonprincipal cells in the guinea pig MSO slice. *J. Neurophysiol.* 73, 1653–1667.
- Smith, P. H., Joris, P. X., and Yin, T. C. 1993. Projections of physiologically characterized spherical bushy cell axons from the cochlear nucleus of the cat: evidence for delay lines to the medial superior olive. *J. Comp. Neurol.* 331, 245–260.
- Smith, P. H., Joris, P. X., and Yin, T. C. 1998. Anatomy and physiology of principal cells of the medial nucleus of the trapezoid body (MNTB) of the cat. *J. Neurophysiol.* 79, 3127–3142.
- Song, P., Yang, Y., Barnes-Davies, M., et al. 2005. Acoustic environment determines phosphorylation state of the Kv3.1 potassium channel in auditory neurons. *Nat. Neurosci.* 8, 1335–1342.
- Spirou, G. A., Rowland, K. C., and Berrebi, A. S. 1998. Ultrastructure of neurons and large synaptic terminals in the lateral nucleus of the trapezoid body of the cat. *J. Comp. Neurol.* 398, 257–272.
- Spitzer, M. W. and Semple, M. N. 1995. Neurons sensitive to interaural phase disparity in gerbil superior olive: diverse monaural and temporal response properties. *J. Neurophysiol.* 73, 1668–1690.
- Spitzer, M. W. and Semple, M. N. 1998. Transformation of binaural response properties in the ascending auditory pathway: influence of time-varying interaural phase disparity. *J. Neurophysiol.* 80, 3062–3076.
- Stotler, W. A. 1953. An experimental study of the cells and connections of the superior olivary complex of the cat. *J. Comp. Neurol.* 98, 401–431.
- Sullivan, W. E. and Konishi, M. 1986. Neural map of interaural phase difference in the owl's brainstem. *Proc. Natl. Acad. Sci. USA* 83, 8400–8404.
- Svirskis, G., Dodla, R., and Rinzel, J. 2003. Subthreshold outward currents enhance temporal integration in auditory neurons. *Biol. Cybern.* 89, 333–340.
- Svirskis, G., Kotak, V., Sanes, D. H., and Rinzel, J. 2002. Enhancement of signal-to-noise ratio and phase locking for small inputs by a low-threshold outward current in auditory neurons. *J. Neurosci.* 22, 11019–11025.
- Svirskis, G., Kotak, V., Sanes, D. H., and Rinzel, J. 2004. Sodium along with low-threshold potassium currents enhance coincidence detection of subthreshold noisy signals in MSO neurons. *J. Neurophysiol.* 91, 2465–2473.
- Thompson, A. M. and Schofield, B. R. 2000. Afferent projections of the superior olivary complex. *Microsc. Res. Tech.* 51, 330–354.
- Tollin, D. J. 2003. The lateral superior olive: a functional role in sound source localization. *Neuroscientist* 9, 127–143.
- Trussell, L. O. 1997. Cellular mechanisms for preservation of timing in central auditory pathways. *Curr. Opin. Neurobiol.* 7, 487–492.
- Trussell, L. O. 1999. Synaptic mechanisms for coding timing in auditory neurons. *Annu. Rev. Physiol.* 61, 477–496.
- Viete, S., Pena, J. L., and Konishi, M. 1997. Effects of interaural intensity difference on the processing of interaural time difference in the owl's nucleus laminaris. *J. Neurosci.* 17, 1815–1824.
- von Bartheld, C. S., Code, R. A., and Rubel, E. W. 1989. GABAergic neurons in brainstem auditory nuclei of the chick: distribution, morphology, and connectivity. *J. Comp. Neurol.* 287, 470–483.
- Wang, L. Y., Gan, L., Forsythe, I. D., and Kaczmarek, L. K. 1998. Contribution of the Kv3.1 potassium channel to high-frequency firing in mouse auditory neurones. *J. Physiol.* 509(Pt 1), 183–194.
- Westerberg, B. D. and Schwarz, D. W. 1995. Connections of the superior olive in the chicken. *J. Otolaryngol.* 24, 20–30.
- Wightman, F. L. and Kistler, D. J. 1993. Sound Localization. In: *Human Psychophysics* (eds. W. A. Yost, A. N. Popper, and R. R. Fay), pp. 155–192. Springer.
- Yang, L., Monsivais, P., and Rubel, E. W. 1999. The superior olivary nucleus and its influence on nucleus laminaris: a source of inhibitory feedback for coincidence detection in the avian auditory brainstem. *J. Neurosci.* 19, 2313–2325.
- Yin, T. C. and Kuwada, S. 1983a. Binaural interaction in low-frequency neurons in inferior colliculus of the cat. III. Effects of changing frequency. *J. Neurophysiol.* 50, 1020–1042.
- Yin, T. C. and Kuwada, S. 1983b. Binaural interaction in low-frequency neurons in inferior colliculus of the cat. II. Effects of changing rate and direction of interaural phase. *J. Neurophysiol.* 50, 1000–1019.
- Yin, T. C. and Chan, J. C. 1990. Interaural time sensitivity in medial superior olive of cat. *J. Neurophysiol.* 64, 465–488.
- Young, S. R. and Rubel, E. W. 1983. Frequency-specific projections of individual neurons in chick brainstem auditory nuclei. *J. Neurosci.* 3, 1373–1378.
- Zhang, S. and Trussell, L. O. 1994. Voltage clamp analysis of excitatory synaptic transmission in the avian nucleus magno-cellularis. *J. Physiol.* 480(Pt 1), 123–136.